Discharge of Inductively Coupled Plasma at Different Thicknesses

Wenyuan Zhang$^{(\boxtimes)}$, Haojun Xu, Xiaolong Wei, and Binbin Pei

Science and Technology on Plasma Dynamics Laboratory, Air Force Engineering University, Xi'an 710038, China
751746892@qq.com

Abstract. Plasma stealth technology has the characteristics of an adjustable wave absorption band, which is a new stealth technology with wider application prospects. The geometry of the cavity is an important external condition that affects the plasma discharge characteristics, while the thickness of the cavity directly determines the transmission distance of radar waves in the plasma, and a decrease in thickness will reduce the attenuation effect of the plasma on electromagnetic waves. In this paper, the effect of cavity thickness on the discharge characteristics of inductively coupled plasma (ICP) is studied, and the fluid model of inductively coupled plasma is established by the multi-physics field coupling method to obtain the distribution laws of n_e and T_e in ICP discharge. The heating electric field of n_e is influenced by the coil structure, the peak region of n_e is concentrated in the geometric center of the cavity for larger thickness, and the electron density increases with the increase of the discharge power. The results have important reference significance for the application of plasma technology in the local stealth of aircraft.

Keywords: Inductively Coupled Plasma · Plasma Discharge · Fluid Model

1 Introduction

The planar type inductively coupled plasma source has a wide operating air pressure, high electron density, large discharge area, and simple device structure, and has outstanding potential advantages in the direction of plasma stealth. When wave-transparent cavity plasma is applied to absorb radar waves, the thinner the cavity, the better it is for installation and use in special areas such as aircraft fuselage surfaces, so the effect of cavity thickness on the discharge characteristics of ICP is investigated in this paper.

The study of plasma stealth technology dates back to 1957 when scientists in the former Soviet Union observed that the electromagnetic scattering properties of artificial satellites under the influence of a plasma layer were different from those of ordinary metal spheres. During the Cold War in the last century, both the United States and the former Soviet Union observed the "black barrier" effect on radar waves by the formation of hundreds of kilometers of plasma regions during low-altitude nuclear explosion tests [1]. In 1962, Swarner published the first research article on the application of plasma

to target RCS reduction [2]. After the 1980s and 1990s, with the rapid development of plasma sources, plasma for attenuation of electromagnetic waves entered a breakthrough stage of development, the most famous experiment was observed in Hughes Lab in 1992 in the 4 ~ 14 GHz band, the RCS attenuation of 13 cm long microwave reflector by plasma generated in a ceramic cover reached 2025 dB [3]. Since then, research related to plasma stealth technology has entered an explosive phase of development.In July 2010, the T-50 fighter jet completed flight tests on the outskirts of Moscow, and related reports claimed that the fighter jet used electron beam plasma stealth technology with electron beam vents installed at the inlet of the air intakes [4]. For the diagnosis of the plasma parameters, several related studies have been carried out [5, 6]. Jingfeng [7] has proposed an effective method to measure the plasma parameters without the interference of the fluctuating electric field and studied the characteristics of the hollow alternating current helium glow discharge. Rui [8] has studied the characteristics of DBD micro-discharge at a different pressure. Tabaie [9] has studied a dielectric barrier discharge device producing atmospheric argon plasma needle and used spectroscopy to calculate the plasma parameters.

In this paper, the simulation study of inductively coupled plasma discharge at different thicknesses is carried out for the stealth requirements of thin wave-transparent cavities applied to local parts of aircraft, and it is found that the plasma distribution generated within the cavities at different thicknesses is different, and the results of the study can provide a reference basis for the stealth application of plasma in local parts of aircraft.

2 Plasma Discharge Simulation Model

Fluid dynamics modeling is one of the common methods used in current numerical simulations of low-temperature plasmas. The fluid model includes the particle continuity equation, the momentum conservation equation, the electron energy equation, and the Poisson equation. Among them, the continuity equations for the density of various types of particles in a plasma discharge are as follows.

$$\frac{\partial n_{e,i,neu}}{\partial t} + \nabla \cdot \Gamma_{e,i,neu} = R_{e,i,neu} \tag{1}$$

where the subscripts e, i, and neu represent electrons, ions, and neutral particles, respectively; n denotes the particle number density; R denotes the corresponding source term for each reactant particle; and Γ is the flux density of each type of particle, derived from the law of conservation of momentum. Under the drift-diffusion approximation, this is given by the following equation.

$$\Gamma_{e,i} = \mp n_{e,i}\mu_{e,i}E - D_{e,i}\nabla n_{e,i} \tag{2}$$

$$\Gamma_{neu} = -D_{neu}\nabla n_{neu} \tag{3}$$

where μ and D are the mobility and diffusion coefficients of the particles, respectively, and the negative and positive signs in the first term on the right side of Eq. (2) apply to electrons and ions, respectively.

The electron energy can be obtained by solving the Electron Energy Equation.

$$\frac{\partial n_\varepsilon}{\partial t} + \nabla \cdot \Gamma_\varepsilon = R_\varepsilon - \Gamma_e \cdot E \tag{4}$$

$$\Gamma_\varepsilon = -(\mu_\varepsilon \cdot E)n_\varepsilon - D_\varepsilon \cdot \nabla n_\varepsilon \tag{5}$$

where n_ε is the electron energy density; R_ε is the electron energy change due to inelastic collisions; $\Gamma_e \cdot E$ is the electron energy obtained by electric field acceleration (Joule heating); Γ_ε is the electron energy flux, μ_ε and D_ε are the mobility and diffusion coefficient of electron energy in space, respectively.

For the spatial electric field strength E, it can be described by Poisson's equation.

$$\nabla \cdot E = -\frac{e(n_i - n_e)}{\varepsilon_0} \tag{6}$$

where ε_0 is the dielectric constant of the working gas.

(a) Plasma model in COMSOL   (b) Plasma profiling grid
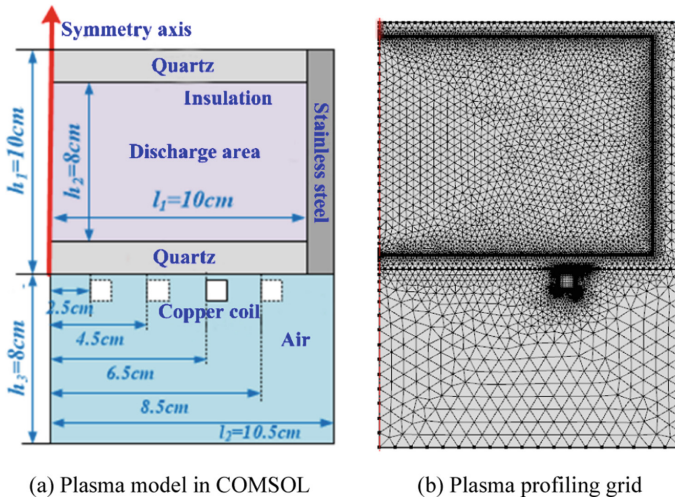
Fig. 1. Geometry and mesh section of the fluid model of the wave-transparent cavity ICP

In this paper, the fluid model is built using the plasma fluid module of the COMSOL Multiphysics platform, and the geometry of the transmissive cavity ICP is referenced in the experimental setup, as shown in Fig. 1 (a). The coil antenna is set up as a solid copper tube with a diameter of 6 mm, the thickness of the dielectric window is 1 cm and the material is quartz, the thickness of the cavity wall is 0.5 cm and the material is stainless steel.

The grid profile is shown in Fig. 1(b). The initial electron number density n_{e0} and the initial average electron energy ε_0 need to be set in the model, and reasonable initial conditions are helpful to improve the iteration speed of the model. n_{e0} and ε_0 were set to 10^9 cm^{-3} and 5 eV, respectively, and the temperature was set to 297 K. The coil antenna was used in power excitation mode with power values consistent with the forward power of the experimental power source.

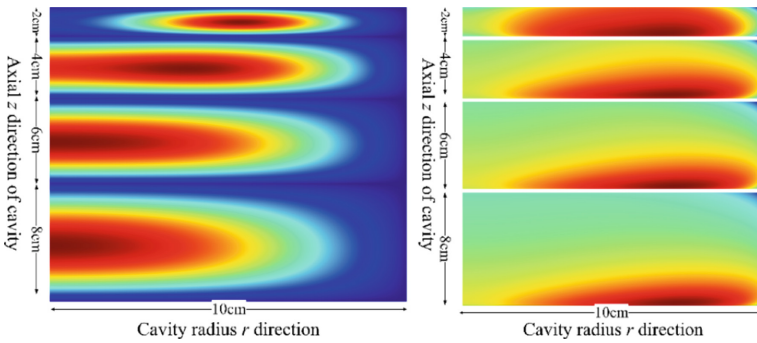## 3   Discharge Simulation and Experimental Results

Fig. 2. Variation of ne and Te distribution with cavity thickness at 10 Pa, z-r cross section

The effect of different cavity thicknesses on the distribution of characteristic parameters was studied by using the established hydrodynamic model. 2 cm, 4 cm, 6 cm and 8 cm cavity thicknesses were selected, the discharge gas was Ar, the discharge pressure was 10 Pa, the discharge power was 300–600 W, and other discharge conditions were kept constant. The effect of thickness change on ne and Te distribution at 10 Pa is given in Fig. 2. When the ICP thickness decreases from 8 cm to 2 cm, the peak region of ne starts to deviate from the center of the cavity, and the deviation distance increases as the thickness decrease. When the thickness is reduced to 2 cm, the peak area of ne moves to the area directly above the coil antenna. At the same power, ne increases with decreasing thickness, while the distribution of Te is similar for different thicknesses, and the effect of thickness on the electron temperature is not significant.

The analysis suggests that at a pressure of 10 Pa, the plasma has moved out of the Langmuir state and random heating dominates in the power absorption mode. Due to the electromagnetic shielding effect, the RF electric field intensity is small in the area above the skinning layer. In contrast, the RF electric field at the cavity axis (r = 0 m) increases with decreasing thickness, so the peak region of the bipolar potential moves toward the region above the skinning layer, and the central region of ne continues to deviate from the cavity center with decreasing thickness, while electrons are heated within the skinning layer and are bounced back to the main plasma region so that ne is lower in the skinning layer.

In order to compare the effect of thickness variation on n_e distribution more visually, Ar-ICP discharge tests were carried out in a transmissive cavity with a quartz cavity thickness of 4 cm and 2 cm, and microwave interference transmission was used to diagnose ne. It is observed that the ICP discharge morphology changes significantly as the cavity thickness decreases, which mainly shows that the thinner the cavity and the higher the air pressure, the more obvious the annular characteristics of the plasma, and the radial width of the annular plasma widens with the increase of power, which is consistent with the trend of plasma morphology changes predicted by the fluid model.
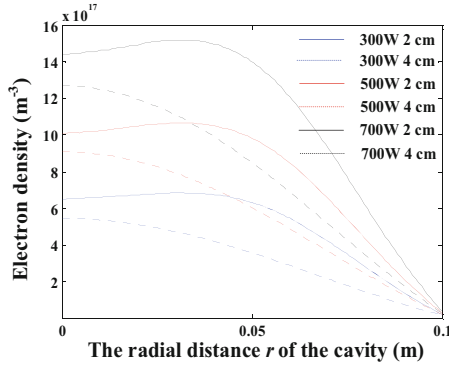
Fig. 3. Comparison of radial results at different thicknesses in 10 Pa
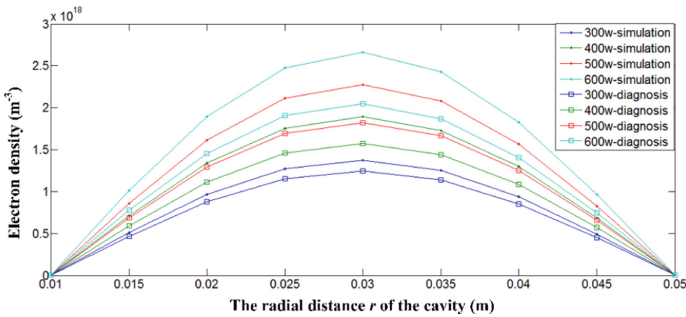

Fig. 4. Variation of electron density with power for a cavity of 4 cm

Figure 3 gives the results of the radial ne comparison under different thickness conditions at 10 Pa. The effective improvement of ne with the reduction of thickness is due to the reduction of cavity volume resulting in more power energy obtained per unit volume of ICP at the same discharge power, and its peak value increases from 9.56×10^{17} m^{-3} to 1.47×10^{18} m^{-3}.

Figure 4 shows the radial comparison results for different power conditions at 4 cm thickness. Overall the electron density increases as the discharge power increases, with the peak electron density about doubling as the power increases from 300 W to 600 W. The analysis suggests that as the power increases, the energy coupled into the cavity by the discharge coil also increases, leading to an increase in the density of the plasma produced by the excitation. Comparing the simulation results with the experimental results for the same power case, it is found that the peak electron density of the experimental results is lower than that of the numerical simulation results. It is analyzed that the reason for this phenomenon is that during the numerical simulation, the power loss and other phenomena existing in the experimental process are not taken into account, resulting in low experimental results, but the overall trend remains consistent and the results of both are in good agreement.

4   Conclusion

For localized plasma cloaking of aircraft, especially on the surface of the airframe or inside the air intakes, the thin-layer wave-transparent cavity ICP discharge technology has a greater potential for engineering applications. In this paper, the discharge of inductively coupled plasma at different thicknesses is studied, and the results of experiments and numerical simulations describe the trend of n_e space variation in agreement. The experimental measurements of n_e are lower than the fluid model results, and the established fluid model can reflect the spatial distribution of n_e more accurately. When the thickness is large, the n_e of ICP is distributed axially. The electrons first gain energy in the heated electric field near the coil, and as the low-energy electrons are expelled from the skinning layer, the peak region of ne moves directly above the heated field region, and the potential distribution in space also changes simultaneously with the diffusion migration of electrons, and after reaching the steady state, n_e reaches its maximum in the geometric center of the cavity. Since the external power provides the energy for plasma excitation, the electron density increases with the increase of the discharge power.

References

1. Sollfrey, W., et al.: Effets of propagation on high-frequency electromagnetic radiation from low-altitude nuclear explosions. Proc. IEEE. **53**, 2035 (1965)
2. Swarner, W.G., Peters, L.: Radar cross sections of dielectric or plasma coated conducting spheres and circular cylinders. IEEE. T. Antenn. Propag. **11**(5), 558–569 (1963)
3. Gregoire, D.J., Santoru, J., Schumacher, R.W.: Electromagnetic-Wave Propagation in Unmagnetized Plasma. AD-A 250710. (1992)
4. Pinglan, W., Liping, H.: Development of plasma technology for stealth. Missiles and Space Vehicles **5**, 008 (2009)
5. Adams, S.F., Bogdanov, E.A., Demidov, V.I., Koepke, M.E., Kudryavtsev, A.A., Williamson, J.M.: Metastable atom and electron density diagnostic in the initial stage of a pulsed discharge in Ar and other rare gases by emission spectroscopy. Physics of Plasmas **19**(2) (2012)
6. Engeln, R., Klarenaar, B., Guaitella, O.: Foundations of optical diagnostics in low-temperature plasmas. Plasma Sources Sci. Technol. **29**(6) (2020)
7. Yao, J., Yuan, C., Yu, Z., Zhou, Z., Kudryavtsev, A.: Measurements of plasma parameters in a hollow electrode AC glow discharge in helium. Plasma Science and Technol. **22**(3) (2020)
8. Liu, R., Yu, Z., Cao, H., Liu, P., Zhang, Z.: Characteristics of DBD micro-discharge at different pressure and its effect on the performance of oxygen plasma reactor. Plasma Science and Technol. **21**(5) (2019)
9. Tabaie, S.S., Iraji, D., Amrollahi, R.: Measurement of electron temperature and density of atmospheric plasma needle. Vacuum **182**, 109761 (2020)